

# Ultra-compact structure in radio quasars as a cosmological probe: a revised study of the interaction between cosmic dark sectors

Xiaogang Zheng,<sup>1,2</sup> Marek Biesiada,<sup>1,2</sup> Shuo Cao,<sup>1</sup> Jingzhao Qi,<sup>1</sup>  
Zong-Hong Zhu<sup>1</sup>

<sup>1</sup> Department of Astronomy, Beijing Normal University, Beijing 100875, China

<sup>2</sup> Department of Astrophysics and Cosmology, Institute of Physics, University of Silesia, Uniwersytecka 4, 40-007 Katowice, Poland

**Abstract.** A new compilation of 120 angular-size/redshift data for compact radio quasars from very-long-baseline interferometry (VLBI) surveys motivates us to revisit the interaction between dark energy and dark matter with these probes reaching high redshifts  $z \sim 3.0$ . In this paper, we investigate observational constraints on different phenomenological interacting dark energy (IDE) models with the intermediate-luminosity radio quasars acting as individual standard rulers, combined with the newest BAO and CMB observation from *Planck* results acting as statistical rulers. The results obtained from the MCMC method and other statistical methods including Figure of Merit and Information Criteria show that: (1) Compared with the current standard candle data and standard clock data, the intermediate-luminosity radio quasar standard rulers, probing much higher redshifts, could provide comparable constraints on different IDE scenarios. (2) The strong degeneracies between the interaction term and Hubble constant may contribute to alleviate the tension of  $H_0$  between the recent *Planck* and *HST* measurements. (3) Concerning the ranking of competing dark energy models, IDE with more free parameters are substantially penalized by the BIC criterion, which agrees very well with the previous results derived from other cosmological probes.

**Keywords:** expansion history – cosmology: observations – methods: statistical

---

## Contents

<b>1</b>	<b>Introduction</b>	<b>1</b>
<b>2</b>	<b>The interacting dark energy models</b>	<b>3</b>
<b>3</b>	<b>Observational data and methodology</b>	<b>4</b>
3.1	Individual standard rulers: QSO	4
3.2	Statistical standard rulers: CMB and BAO	5
3.3	Alternative standard probes for comparison: SN Ia and $H(z)$	7
<b>4</b>	<b>Results and discussion</b>	<b>9</b>
<b>5</b>	<b>Conclusions</b>	<b>13</b>
<b>6</b>	<b>Acknowledgments</b>	<b>14</b>

---

## 1 Introduction

Dark energy has become one of the most important issues of modern cosmology since many astrophysical and cosmological observations such as Type Ia Supernovae (SN Ia) [1, 2], Large Scale Structure (LSS) [3] and cosmic microwave background radiation (CMB) [4] coherently indicate that the universe is undergoing an accelerated expansion at the present stage. The most simple candidate for the uniformly distributed material component responsible for this behaviour, is some form of vacuum energy density or cosmological constant  $\Lambda$ . Despite its simplicity, the simple cosmological constant is always entangled with the well-known coincidence problem: the matter density  $\rho_m$  decreases with the expansion of the universe as  $a^{-3}$  and the density of cosmological constant  $\rho_\Lambda$  does not change with the expansion of the universe, whereas the matter density is comparable with the dark energy density today. More recent works have implied that this simple  $\Lambda$ CDM model encounters other problems. For instance, a tension between  $\Lambda$ CDM and the measurements of Hubble parameter ( $H(z)$ ) has been extensively discussed in the framework of different  $Om$  diagnostics [5–7]. Moreover, the local measurement of Hubble constant ( $H_0$ ) through the Wide Field Camera 3 (WFC3) on the Hubble Space Telescope (*HST*) [8] suggests a higher value of  $H_0$  than the prediction of  $\Lambda$ CDM model from *Planck* CMB data [9]. In order to meet these problems, the consideration of the possibility of exchanging energy between DE and DM through an interaction term seems feasible, as the coupling between these dark sectors can provide a mechanism to alleviate the coincidence problem [10–12] and provide possible a larger value of  $H_0$  derived from the recent *HST* measurement.

However, the nature of DE and DM remains a mystery and most of the investigation of interaction is based on the phenomenological assumptions. As extensively considered in the literature (see e.g. Dalal et al. [13], Guo et al. [14], Li et al. [15]), we assume that dark energy and dark matter exchange energy through an interaction term  $Q$ , while there is no

interaction between baryonic matter and dark energy

$$\begin{aligned}\dot{\rho}_X + 3H(\rho_X + p_X) &= -Q, \\ \dot{\rho}_c + 3H\rho_c &= Q, \\ \dot{\rho}_b + 3H\rho_b &= 0.\end{aligned}\tag{1.1}$$

where  $\rho_X$ ,  $\rho_c$  and  $\rho_b$  denote the energy density of dark energy, cold dark matter and baryonic matter, respectively. In fact, in the standard model of particle physics combined with the solar system experiments [16], the coupling between dark energy and baryons is basically constrained to irrelevantly small values. This is in agreement with the results obtained in the modified interacting dark energy (MIDE) model as a candidate to describe possible interaction between dark energy and dark matter as well as that between dark energy and baryonic matter [17].

Note that with the ansatz (1.1), the total energy density is conserved:  $\dot{\rho}_{tot} + 3H(\rho_{tot} + p_{tot}) = 0$ . If  $Q$  is a non-zero function of the scale factor, the interaction makes  $\rho_m$  and  $\rho_X$  to deviate from the standard scaling. Considering from continuity equations, the interaction term  $Q$  must be a function multiplied by the energy density and a quantity said the inverse of time which can be considered by the Hubble factor  $H$ . The simplest assumptions including a freedom of choice concerning the form of the energy density are  $Q = Q(H\rho_c)$  and  $Q = Q(H\rho_X)$  (see Cao et al. [18] and references therein). We assume that, for the phenomenological interaction models, the equation of state (EoS) of dark energy  $w_X \equiv p/\rho$  is constant in spatially flat FRW metric. The standard cosmology without interaction between dark energy and dark matter is recovered with  $Q = 0$ , while  $Q \neq 0$  denotes non-standard cosmology. On the other hand, the value of  $Q$  determines the extent of interaction and transfer direction between dark energy and dark matter, i.e.,  $Q < 0$  indicates that the energy is transferred from dark matter to dark energy, while  $Q > 0$  denotes that the energy is transferred from dark energy to dark matter.

In the previous works, different interacting dark energy models have been discussed with various cosmological observations [18–23]. Recently, the angular size of compact structure in radio quasars versus redshift data from the very-long-baseline interferometry (VLBI) observations have become an effective probe in cosmology and astrophysics [24, 25]. Based on a 2.29 GHz VLBI all-sky survey of 613 milliarcsecond ultra-compact radio sources, Cao et al. [25] extracted a sub-sample of 120 intermediate-luminosity quasars in the redshift range of  $0.46 < z < 2.8$ , which can be used as cosmological standard rulers with the linear sizes calibrated by a cosmological-model-independent method. Compared with the commonly-used SN Ia standard candles ( $z \sim 1.4$ ), the advantage of this data set is that quasars are observed at much higher redshifts ( $z \sim 3.0$ ), which motivates us to investigate the possible interaction between dark energy and dark matter at higher redshifts. To reduce the uncertainty and put tighter constraint on the value of the coupling, we add, in our discussion, the CMB observation from the *Planck* results as well as the BAO measurements both from the low- $z$  Galaxy and higher- $z$  Lyman- $\alpha$  Forests (Ly $\alpha$ F) data. We expect that sensitivities of measurements of different observables can give complementary results on the coupling between dark sectors.

This paper is organized as follows: The Friedmann equations in the IDE models are presented in Section 2. In Section 3, we introduce the observational data including QSO, BAO and CMB and the corresponding methodology. In Section 4, we perform a Markov Chain Monte Carlo (MCMC) analysis, and furthermore apply the Figure of Merit (FoM) and two model selection techniques, i.e., the Akaike Criterion (AIC) and Bayesian Information Criterion (BIC). Finally the results are summarized in Section 5.

## 2 The interacting dark energy models

In this paper, in order to derive stringent constraints on the interaction between DE and DM, having in mind the well known degeneracy between model parameters, we assume a flat universe which is strongly supported by CMB data. In a zero-curvature universe filled with ordinary pressureless dust matter (cold dark matter plus baryons), radiation and dark energy, the Friedmann equation reads

$$\rho = \rho_b + \rho_c + \rho_X + \rho_r = 3H^2(z)/8\pi G \quad (2.1)$$

where  $\rho_r$  is the energy density of radiation. We remark here that the effect of this radiation term, which is negligible for low- $z$  observations, should be taken into account when considering the redshifts at photo-decoupling epoch  $z_*$  and baryon-drag epoch  $z_d$  for the comoving sound horizon in CMB and BAO. Obviously, the dimensionless expansion rate of the Universe,  $E(z)$ , without the interaction between dark matter and dark energy can be expressed as

$$E^2(z; \mathbf{p}) = (\Omega_{b0} + \Omega_{c0})(1+z)^3 + \Omega_{r0}(1+z)^4 + \Omega_X(z). \quad (2.2)$$

where  $\Omega_{b0} = (8\pi G\rho_{b0})/(3H_0^2)$  is the current baryonic matter component,  $\Omega_{c0} = (8\pi G\rho_{c0})/(3H_0^2)$  is the current dark matter component, the current radiation component  $\Omega_{r0} = (8\pi G\rho_{r0})/(3H_0^2) = 4.1736 \times 10^{-5}h^{-2}$  [26], and the dark energy component

$$\Omega_X(z) = (1 - \Omega_{b0} - \Omega_{c0} - \Omega_{r0}) \times (1+z)^{3(1+w)}. \quad (2.3)$$

In our analysis, we assume that dark energy and cold dark matter exchange energy through interaction term  $Q$  proportional to different energy densities  $\rho_i$ , i.e.,  $Q = 3\gamma_i H \rho_i$ , where  $\gamma_i$  is a dimensionless constant. The simplest assumption with the freedom to choose the form of the energy density are

$$Q_1 = 3\gamma_c H \rho_c \quad (2.4)$$

and

$$Q_2 = 3\gamma_X H \rho_X, \quad (2.5)$$

where the constants  $\gamma_c$  and  $\gamma_X$  quantify the extent of interaction between cold dark matter and dark energy. Correspondingly,  $\gamma_i = 0$  indicates that there is no interaction between dark energy and dark matter, while the energy is transferred from dark matter to dark energy when  $\gamma_i < 0$ , and from dark energy to dark matter when  $\gamma_i > 0$ . For the first case, the interaction term  $Q$  is proportional to the energy density of cold dark matter  $\rho_c$ . Combining Eq.(1.1) and the corresponding expression of Eq.(2.4), we obtain the energy density of dark matter and dark energy as  $\rho_c = \rho_{c0}(1+z)^{3(1-\gamma_c)}$  and  $\rho_X = C(1+z)^{3(1+w) - \frac{\gamma_c \rho_{c0}}{\gamma_c + w}(1+z)^{3(1-\gamma_c)}}$ , where  $C$  is an integral constant to be determined. From the Friedmann equation ( $H^2(z) = 8\pi G(\rho_b + \rho_c + \rho_X + \rho_r)/3$ ) combined with  $H_0^2 = 8\pi G\rho_{cr}/3$ , the Hubble parameter for this interacting dark energy model (which is denoted as  $\gamma_c$ IwCDM model hereafter) is written as

$$E^2(z) = \frac{w\Omega_{c0}}{\gamma_c + w}(1+z)^{3(1-\gamma_c)} + \Omega_{b0}(1+z)^3 + \Omega_{r0}(1+z)^4 + (1 - \Omega_{b0} - \Omega_{r0} - \frac{w\Omega_{c0}}{\gamma_c + w})(1+z)^{3(1+w)}. \quad (2.6)$$

It can be seen that vanishing interaction term  $\gamma_c = 0$ , corresponds to the well-known wCDM parametrization. Moreover, in our analysis we will consider another special case of the

$\gamma_c$ IwCDM model with  $w = -1$ , i.e., the possibility that the cosmological constant (vacuum energy) exchange energy with dark matter through an interaction term  $\gamma_c$ , which is denoted as  $\gamma_c$ IACDM model hereafter. For the second case, when the interaction is proportional to the dark energy density  $\rho_X$  (which is denoted as  $\gamma_X$ IwCDM model hereafter), the dimensionless expansion rate of the Universe reads

$$E^2(z) = \frac{w(\Omega_{b0} + \Omega_{c0}) + \gamma_X}{w + \gamma_X}(1+z)^3 + \Omega_{r0}(1+z)^4 + \frac{w(1 - \Omega_{b0} - \Omega_{c0})}{w + \gamma_X}(1+z)^{3(1+w+\gamma_X)}. \quad (2.7)$$

which corresponds to the  $\gamma_X$ IACDM model with  $w = -1$ .

Let us emphasize the use of the Hubble constant  $H_0$  in our analysis. Considering the tension of its precise value between different astrophysical methods, i.e., Cepheids from the Hubble Space Telescope (*HST*) key project [8] and CMB data from the *Planck* satellite experiment [27], we will keep the Hubble constant as a free parameter, which will be constrained by the observational data described below. Therefore, the interacting dark energy models considered in this paper have five parameters ( $\Omega_{b0}$ ,  $\Omega_{c0}$ ,  $w$ ,  $\gamma_i$  and  $H_0$ ), where  $\Omega_{b0}$  and  $\Omega_{c0}$  specify the current density of baryonic matter and dark matter,  $w$  denotes the equation of state of dark energy,  $\gamma_c$  and  $\gamma_X$  presents how strongly dark energy interacts with dark matter.

### 3 Observational data and methodology

In this work, we will consider a combination of three types of standard rulers to derive the information of angular diameter distances and thus the interaction between dark sectors at different redshifts, i.e., the compact radio quasars data from VLBI, the cosmic microwave background (CMB) measurements from the *Planck* results, and the baryonic acoustic oscillations (BAO) from the low- $z$  galaxy data and the higher- $z$  Lyman- $\alpha$  Forests (Ly $\alpha$ F) data. The first probes can be considered as individual standard rulers while the other two probes are treated as statistical standard rulers in cosmology. For comparison, we also considered two more standard probes alternative to standard rulers: standard candles – type Ia supernovae (SN Ia) and standard chronometers – passively evolving galaxies (more precisely,  $H(z)$  data derived from them).

#### 3.1 Individual standard rulers: QSO

It is well known that for objects with determined intrinsic physical size, one can determine the corresponding angular diameter distances by measuring their angular sizes at different redshifts. In the case of compact radio-sources used here, characteristic angular size obtained from VLBI has been obtained as

$$\theta = \frac{2\sqrt{-\ln\Gamma\ln 2}}{\pi B} \quad (3.1)$$

where  $B$  is the interferometer baseline and the visibility modulus  $\Gamma$  is the ratio of the total flux density  $S_{tot}$  and correlated flux density  $S_{corr}$  [32]. We note that all quantities derived from the  $S_{corr}/S_{tot}$  ratio (including the apparent angular size) are weakly dependent on the source orientation, considering the well-known fact that for most of the strongly core dominated radio sources the viewing angle should be close to the  $1/\gamma_{jet}$  value. Angular sizes of the compact structure  $\theta_{obs}$  and their corresponding uncertainties  $\sigma_\theta(z_i)$  (comprising both statistical and systematical uncertainty) can be found in [24]. As is extensively discussed in

the literature [28], the linear sizes of compact structure in radio sources could depend on the luminosity and redshift as

$$l_m = lL^\beta(1+z)^n \quad (3.2)$$

where  $\beta$  and  $n$  are the two parameters respectively characterizing the “linear size - luminosity” and “linear size - redshift” relations. Let us recall that besides cosmological evolution of the linear size with redshift, the parameter  $n$  may also characterize the dependence of the linear size on the emitted frequency, as well as image blurring due to scattering in the propagation medium.

The possibility to alleviate the dependence of  $l_m$  on the source luminosity and redshift were discussed early by Gurvits, Kellerman & Frey [29], Vishwakarma [30]. Then Cao et al. [31] using a compilation of mixed population of radio sources including different optical counterparts found they can not act as standard ruler. Most recently, the analysis of [24] indicated that only a sub-sample of intermediate-luminosity radio quasars ( $10^{27}$  W/Hz  $< L < 10^{28}$  W/Hz) displayed negligible dependence on luminosity and redshift ( $\beta \simeq 10^{-4}$ ,  $|n| \simeq 10^{-3}$ ) and therefore could serve as a standard ruler in cosmology. Let us stress that sample selection in terms of luminosity, which involves the knowledge of angular diameter distances to the quasars, can be performed in a robust way not depending on the details of cosmological model (for details see [24]) and does not induce circularity problems in using QSOs for cosmological model parameter inference. Cao et al. [25] also confirmed that the uncertainties of  $\beta$  and  $n$  do not influence the best-fit cosmological parameters noticeably. For the observational quasar data, we adopt the measurements of 120 intermediate-luminosity radio quasars in the redshift range  $0.46 < z < 2.80$ . In previous works, the intrinsic linear size  $l_m$  was calibrated using the angular diameter distances estimated from two different methods: the supernova distance modulus [24] and the cosmic chronometers (themselves being cosmology-independent probe) using a robust reconstruction technique called the Gaussian process [25]. In this paper, we choose to use the linear size of this standard ruler calibrated as  $l_m = 11.03 \pm 0.25$  pc through the cosmological-model-independent method [25]. The angular size of the compact structure in intermediate-luminosity radio quasars, observed at redshifts  $z$ , can be theoretically expressed as

$$\theta_{th}(z) = \frac{l_m}{D_A(z)} \quad (3.3)$$

where  $D_A$  is the angular diameter distance computed in the models of interest, which reads

$$D_A(z; \mathbf{p}) = \frac{c}{H_0} \frac{1}{1+z} \int_0^z \frac{dz'}{E(z'; \mathbf{p})} \quad (3.4)$$

in flat Friedman-Robertson-Walker metric.

In order to constrain the model parameters  $\mathbf{p}$  using these quasar data, we define the likelihood function  $\mathcal{L}_{QSO} \propto \exp[-\chi_{QSO}^2(z; \mathbf{p})/2]$ , where  $\chi_{QSO}^2$  is related to the quasar sample as

$$\chi_{QSO}^2 = \sum_{i=1}^{120} \frac{[\theta_{obs}(z_i) - \theta_{th}(z_i; \mathbf{p})]^2}{\sigma_\theta^2(z_i)}. \quad (3.5)$$

### 3.2 Statistical standard rulers: CMB and BAO

The first statistical standard ruler used in our analysis is the cosmic microwave background (CMB), providing the sound horizon scale at high redshift ( $z \sim 1089$ ), useful for determining

the properties of dark sectors in the Universe. For the CMB data, we will use the measurements of several quantities derived from *Planck* [27], which include the acoustic scale ( $l_A$ ), the shift parameter ( $R$ ), and the baryonic matter fraction at the redshift of recombination ( $\Omega_{b0}h^2$ ). Firstly, the acoustic scale is expressed as

$$l_A \equiv (1 + z_*) \frac{\pi D_A(z_*)}{r_s(z_*)} \quad (3.6)$$

where the redshift of photon-decoupling period can be calculated as [33]

$$z_* = 1048[1 + 0.00124(\Omega_{b0}h^2)^{-0.738}][1 + g_1(\Omega_{m0}h^2)^{g_2}] \quad (3.7)$$

$$g_1 = \frac{0.0783(\Omega_{b0}h^2)^{-0.238}}{1 + 39.5(\Omega_{b0}h^2)^{0.763}}, g_2 = \frac{0.560}{1 + 21.1(\Omega_{b0}h^2)^{1.81}} \quad (3.8)$$

The comoving sound horizon can be parameterized as

$$\begin{aligned} r_s(z_*) &= \int_0^{z_*} \frac{c_s dt'}{a} = \frac{c}{H_0} \int_{z_*}^{\infty} \frac{c_s dz}{E(z)} \\ &= \frac{c}{H_0} \int_0^{a_*} \frac{da}{a^2 E(a) \sqrt{3(1 + \bar{R}_b a)}}. \end{aligned} \quad (3.9)$$

with  $\bar{R}_b = 31500(T_{CMB}/2.7K)^{-4}\Omega_{b0}h^2$  and  $T_{CMB} = 2.7255K$ . Note that the current radiation component is related to the matter density as  $\Omega_{r0} = \Omega_{m0}/(1 + z_{eq})$ , where  $z_{eq} = 2.5 \times 10^4 \Omega_{m0} h^2 (T_{CMB}/2.7K)^{-4}$ . Secondly, the other commonly-used CMB shift parameter reads [34]

$$R(z_*) \equiv \frac{(1 + z_*) D_A(z_*) \sqrt{\Omega_{m0} H_0^2}}{c} \quad (3.10)$$

Model parameters can be estimated from the CMB data using the likelihood based on the  $\chi^2$  function defined as

$$\chi_{CMB}^2 = \Delta P_{CMB}^T C_{CMB}^{-1} \Delta P_{CMB} \quad (3.11)$$

where  $\Delta P_{CMB}$  is the difference between the theoretical distance priors and the observational counterparts. The corresponding inverse covariance matrix  $C_{CMB}^{-1}$  can be found in Table. 4 provided by Planck Collaboration XIV [27].

The second statistical standard ruler applied in our analysis is the baryonic acoustic oscillations (BAO) scale, the measurements of which are derived from both the low- $z$  galaxy and higher- $z$  Lyman- $\alpha$  Forests(Ly $\alpha$ F) data. For the lower-redshift BAO observations, we turn to the latest measurements of acoustic-scale distance ratio from the 6-degree Field Galaxy Survey (6dFGS) [35], the 'main galaxy sample' from Sloan Digital Sky Survey (SDSS-MGS) [36], and the two principal Baryon Oscillation Spectroscopic Survey (BOSS) galaxy samples (BOSS-LOWZ and BOSS-CMASS) [37], while for the the higher- $z$  measurement is derived from SDSS DR12 [38]. Now three different types of distance ratios  $D_V(z)/r_s(z_d)$ ,  $D_M(z)/r_s(z_d)$  and  $D_H(z)/r_s(z_d)$  are listed in Table. 1. We remark that  $r_s(z_d)$  is the comoving sound horizon at the baryon-drag epoch  $z_d$  [39]

$$z_d = \frac{1291(\Omega_{m0}h^2)^{0.251}}{1 + 0.659(\Omega_{m0}h^2)^{0.828}} [1 + b_1(\Omega_{b0}h^2)^{b_2}] \quad (3.12)$$



**Table 1.** Distance ratios from recent BAO measurements.

Survey	$z$	$D_V(z)/r_s(z_d)$	$D_M(z)/r_s(z_d)$	$D_H(z)/r_s(z_d)$	Reference
6dFGS	0.106	$3.047 \pm 0.137$	–	–	Beutler et al. [35]
SDSS-MGS	0.15	$4.480 \pm 0.168$	–	–	Ross et al. [36]
BOSS-LOWZ	0.32	$8.594 \pm 0.095$	$8.774 \pm 0.142$	$25.89 \pm 0.76$	Anderson et al. [37]
BOSS-CMASS	0.57	$13.757 \pm 0.142$	$14.745 \pm 0.237$	$21.02 \pm 0.52$	Anderson et al. [37]
SDSS DR12	2.33	–	$37.77 \pm 2.73$	$9.07 \pm 0.31$	Bautista et al. [38]

with

$$\begin{aligned} b_1 &= 0.313(\Omega_{m0}h^2)^{-0.419}[1 + 0.607(\Omega_{m0}h^2)^{0.674}], \\ b_2 &= 0.238(\Omega_{m0}h^2)^{0.223}. \end{aligned} \quad (3.13)$$

$D_V(z)$ ,  $D_M(z)$  and  $D_H(z)$  represent the volume-averaged effective distance ( $[(1+z)^2 D_A^2(z) cz/H(z)]^{1/3}$ ), the comoving angular-diameter distance ( $(1+z)D_A(z)$ ), and the Hubble distance ( $c/H(z)$ ), respectively. The  $\chi^2$  function constructed from the BAO observations is denoted as  $\chi_{BAO}^2$  hereafter and it can be expressed as

$$\chi_{BAO}^2 = \sum_{i=1}^n \frac{(\mathcal{R}_{th} - \mathcal{R}_{obs})^2}{(\Delta \mathcal{R}_{obs})^2} \quad (3.14)$$

where  $\mathcal{R}$  stands for three different types of distance ratios mentioned above.

### 3.3 Alternative standard probes for comparison: SN Ia and $H(z)$

As it is well known, the evidence for cosmic acceleration came first from other type of standard probes in cosmology, i.e., type Ia supernovae (SN Ia) probing the luminosity distance  $D_L$ . Later on, the ages of passively evolving early-type galaxies (cosmic chronometers) became available providing direct measurements of the Hubble parameter  $H(z)$  at different redshifts. In order to compare our QSO fits, with the results obtained using these alternative probes, we also considered the latest Union2.1 compilation [40] consisting of 580 SN Ia in the redshift range  $0.014 < z < 1.415$  and 30 Hubble parameter measurements [7] in the redshift range  $0.07 < z < 1.965$  obtained from cosmic chronometers.

The  $\chi_{SN}^2$  of the Union2.1 SN Ia is given by

$$\chi_{SN}^2 = (\mu_{obs} - \mu_{th})^T C_{SN}^{-1} (\mu_{obs} - \mu_{th}) \quad (3.15)$$

where  $\mu = 5 \log_{10}(D_L/Mpc) + 25$  is the distance modulus and  $C_{SN}$  is the covariance matrix, and the  $\chi_{H(z)}^2$  of the  $H(z)$  data is given by

$$\chi_{H(z)}^2 = \sum_{i=1}^{30} \frac{[H_{obs}(z_i) - H_{th}(z_i; \mathbf{p})]^2}{\sigma_{H_{obs}(z_i)}^2} \quad (3.16)$$

where  $H_{obs}(z_i)$  and  $\sigma_{H_{obs}(z_i)}$  are the 30 Hubble parameter measurements and their uncertainties, respectively.

In the next section we will present the results of joint analysis involving the above mentioned probes in different combinations based on minimizing the following chi-square functions:  $\chi_{C1}^2 = \chi_{CMB}^2 + \chi_{BAO}^2$ ,  $\chi_{C2}^2 = \chi_{QSO}^2 + \chi_{CMB}^2 + \chi_{BAO}^2$ ,  $\chi_{C3}^2 = \chi_{CMB}^2 + \chi_{BAO}^2 + \chi_{SN}^2 + \chi_{H(z)}^2$ , and  $\chi_{C4}^2 = \chi_{QSO}^2 + \chi_{CMB}^2 + \chi_{BAO}^2 + \chi_{SN}^2 + \chi_{H(z)}^2$ . In adopting the MCMC approach, we



generate a chain of sample points distributed in the parameter space according to the posterior probability by using the Metropolis-Hastings algorithm with uniform prior probability distribution, and then repeat this process until the established convergence accuracy can be satisfied. Our code is based on CosmoMC [41] and we generated eight chains after setting  $R - 1 = 0.001$  to guarantee the accuracy of the fits.

**Table 2.** The marginalized  $1\sigma$  uncertainties of the parameters  $\Omega_{b0}$ ,  $\Omega_{c0}$ ,  $w$ ,  $\gamma_i$ , and  $H_0$  for different interacting dark energy scenarios, as well as  $\chi^2/d.o.f$  and  $FoM$ , obtained from the combinations of the data sets C1 (CMB+BAO), C2 (QSO+CMB+BAO), C3 (CMB+BAO+SN+ $H(z)$ ) and C4 (QSO+CMB+BAO+SN+ $H(z)$ ), respectively. Corresponding results for the  $\Lambda$ CDM and  $w$ CDM models are also added for comparison.

$\Lambda$ CDM	$\Omega_{b0}$	$\Omega_{c0}$	$w$	$\gamma$	$H_0$	$\chi^2/d.o.f$	$FoM$
C1	$0.0501^{+0.0011}_{-0.0010}$	$0.277^{+0.011}_{-0.011}$	-1	0	$66.48^{+0.81}_{-0.81}$	10.35/10	$7.33 \times 10^6$
C2	$0.0500^{+0.0010}_{-0.0009}$	$0.276^{+0.010}_{-0.010}$	-1	0	$66.59^{+0.80}_{-0.80}$	364.55/130	$7.37 \times 10^6$
C3	$0.0499^{+0.0009}_{-0.0009}$	$0.275^{+0.008}_{-0.008}$	-1	0	$66.62^{+0.79}_{-0.79}$	571.26/620	$7.91 \times 10^6$
C4	$0.0499^{+0.0009}_{-0.0008}$	$0.275^{+0.008}_{-0.008}$	-1	0	$66.66^{+0.79}_{-0.78}$	925.36/740	$7.96 \times 10^6$
$\gamma_c$ I $\Lambda$ CDM	$\Omega_{b0}$	$\Omega_{c0}$	$w$	$\gamma_c$	$H_0$	$\chi^2/d.o.f$	$FoM$
C1	$0.0487^{+0.0018}_{-0.0015}$	$0.277^{+0.009}_{-0.009}$	-1	$-0.0025^{+0.0027}_{-0.0022}$	$67.75^{+1.25}_{-1.50}$	8.95/9	$2.95 \times 10^9$
C2	$0.0483^{+0.0015}_{-0.0013}$	$0.276^{+0.009}_{-0.009}$	-1	$-0.0029^{+0.0021}_{-0.0018}$	$68.04^{+1.01}_{-1.23}$	361.19/129	$4.73 \times 10^9$
C3	$0.0486^{+0.0014}_{-0.0013}$	$0.276^{+0.009}_{-0.010}$	-1	$-0.0025^{+0.0020}_{-0.0019}$	$67.38^{+0.98}_{-1.06}$	569.12/619	$4.87 \times 10^9$
C4	$0.0485^{+0.0014}_{-0.0012}$	$0.276^{+0.009}_{-0.010}$	-1	$-0.0026^{+0.0018}_{-0.0018}$	$67.88^{+0.92}_{-1.03}$	921.38/739	$5.51 \times 10^9$
$\gamma_X$ I $\Lambda$ CDM	$\Omega_{b0}$	$\Omega_{c0}$	$w$	$\gamma_X$	$H_0$	$\chi^2/d.o.f$	$FoM$
C1	$0.0504^{+0.0011}_{-0.0011}$	$0.276^{+0.010}_{-0.013}$	-1	$-0.0052^{+0.0077}_{-0.0083}$	$66.45^{+1.04}_{-0.71}$	9.16/9	$1.44 \times 10^9$
C2	$0.0504^{+0.0010}_{-0.0010}$	$0.275^{+0.010}_{-0.010}$	-1	$-0.0052^{+0.0077}_{-0.0083}$	$66.53^{+0.81}_{-0.70}$	363.24/129	$1.59 \times 10^9$
C3	$0.0503^{+0.0010}_{-0.0010}$	$0.274^{+0.010}_{-0.010}$	-1	$-0.0052^{+0.0077}_{-0.0082}$	$66.55^{+0.77}_{-0.71}$	570.04/620	$1.63 \times 10^9$
C4	$0.0503^{+0.0010}_{-0.0010}$	$0.274^{+0.009}_{-0.010}$	-1	$-0.0057^{+0.0077}_{-0.0082}$	$66.64^{+0.77}_{-0.70}$	924.07/739	$1.64 \times 10^9$
$w$ CDM	$\Omega_{b0}$	$\Omega_{c0}$	$w$	$\gamma$	$H_0$	$\chi^2/d.o.f$	$FoM$
C1	$0.0517^{+0.0035}_{-0.0024}$	$0.282^{+0.013}_{-0.010}$	$-0.94^{+0.10}_{-0.08}$	0	$65.61^{+1.28}_{-2.03}$	8.86/9	$1.01 \times 10^8$
C2	$0.0515^{+0.0034}_{-0.0024}$	$0.281^{+0.012}_{-0.011}$	$-0.95^{+0.10}_{-0.07}$	0	$65.83^{+1.24}_{-2.01}$	363.29/129	$1.05 \times 10^8$
C3	$0.0502^{+0.0029}_{-0.0020}$	$0.275^{+0.012}_{-0.011}$	$-0.98^{+0.09}_{-0.08}$	0	$66.54^{+1.45}_{-1.53}$	570.96/619	$1.28 \times 10^8$
C4	$0.0500^{+0.0029}_{-0.0020}$	$0.275^{+0.012}_{-0.010}$	$-0.99^{+0.09}_{-0.07}$	0	$66.64^{+1.23}_{-1.73}$	925.13/739	$1.31 \times 10^8$
$\gamma_c$ I $w$ CDM	$\Omega_{b0}$	$\Omega_{c0}$	$w$	$\gamma_c$	$H_0$	$\chi^2/d.o.f$	$FoM$
C1	$0.0509^{+0.0069}_{-0.0066}$	$0.282^{+0.015}_{-0.016}$	$-0.95^{+0.14}_{-0.15}$	$-0.0008^{+0.0044}_{-0.0042}$	$65.96^{+4.69}_{-4.06}$	8.76/8	$1.26 \times 10^{10}$
C2	$0.0483^{+0.0045}_{-0.0040}$	$0.277^{+0.012}_{-0.012}$	$-1.00^{+0.11}_{-0.11}$	$-0.0026^{+0.0026}_{-0.0023}$	$67.96^{+2.79}_{-2.89}$	361.19/128	$4.50 \times 10^{10}$
C3	$0.0481^{+0.0032}_{-0.0033}$	$0.274^{+0.011}_{-0.010}$	$-1.02^{+0.08}_{-0.09}$	$-0.0025^{+0.0025}_{-0.0024}$	$68.26^{+2.62}_{-2.30}$	569.07/618	$5.50 \times 10^{10}$
C4	$0.0476^{+0.0029}_{-0.0026}$	$0.274^{+0.010}_{-0.010}$	$-1.03^{+0.08}_{-0.07}$	$-0.0029^{+0.0019}_{-0.0017}$	$68.62^{+1.71}_{-2.05}$	921.16/738	$8.88 \times 10^{10}$
$\gamma_X$ I $w$ CDM	$\Omega_{b0}$	$\Omega_{c0}$	$w$	$\gamma_X$	$H_0$	$\chi^2/d.o.f$	$FoM$
C1	$0.0514^{+0.0050}_{-0.0041}$	$0.281^{+0.020}_{-0.017}$	$-0.96^{+0.18}_{-0.14}$	$-0.0022^{+0.0135}_{-0.0120}$	$65.83^{+2.46}_{-3.14}$	8.85/8	$6.26 \times 10^9$
C2	$0.0510^{+0.0041}_{-0.0040}$	$0.278^{+0.017}_{-0.016}$	$-0.97^{+0.14}_{-0.15}$	$-0.0042^{+0.0127}_{-0.0109}$	$66.06^{+2.60}_{-2.58}$	363.13/128	$8.08 \times 10^9$
C3	$0.0498^{+0.0030}_{-0.0028}$	$0.274^{+0.014}_{-0.013}$	$-1.03^{+0.12}_{-0.11}$	$-0.0081^{+0.0122}_{-0.0095}$	$66.80^{+1.87}_{-1.88}$	569.97/618	$1.64 \times 10^{10}$
C4	$0.0499^{+0.0028}_{-0.0030}$	$0.273^{+0.013}_{-0.014}$	$-1.02^{+0.11}_{-0.11}$	$-0.0070^{+0.0109}_{-0.0097}$	$66.79^{+2.01}_{-1.73}$	923.94/738	$1.64 \times 10^{10}$

## 4 Results and discussion

In order to demonstrate the constraining power of quasars on the interaction between DE and DM, both individual and joint constraint results will be presented in the following analysis. Firstly, the fitting results from the compact structure measurements of 120 quasars are shown in Fig. 1, in the framework of the  $\gamma_c$  IwCDM and  $\gamma_X$  IwCDM models. For comparison, confidence contours concerning the constraints obtained with QSO, SN and  $H(z)$  individually and in combination are displayed as well. Note that we are focusing on the interaction term between cosmic dark sectors and individual standard probes cannot tightly constrain the matter density parameters. Therefore, we have assumed the best fitted  $\Omega_{b0}$  and  $\Omega_{c0}$  obtained by the recent *Planck* observations [9] as priors. It is clear that the quasar data could provide constraints comparable to the other two types of standard probes, i.e., standard candle (SN Ia) and  $H(z)$  from cosmic chronometers. Moreover, our results displayed in Fig 1 suggest that larger and more accurate sample of the quasar data can be a valuable complementary probe to test the properties of dark energy and break the degeneracy in the IDE model parameters. This tendency will also be preserved in more stringent constraints obtained from the combination of those three probes. Secondly, we compared the performance of statistical standard rulers (CMB+BAO) themselves and combined with other probes (CMB+BAO+SN+ $H(z)$ ) in two settings: with and without inclusion of QSO. Unlike the former case, density parameters  $\Omega_{b0}$  and  $\Omega_{c0}$  could now be fitted reliably and were treated as a free parameters. In order to illustrate the comparison of results between different data sets, we just show the 2-D plots and 1-D marginalized distributions with  $1\text{-}\sigma$  and  $2\text{-}\sigma$  contours of the parameters ( $w$ ,  $\gamma$ , and  $H_0$ ) in Figs. 2-3. Corresponding numerical values of central fits and  $1\sigma$  uncertainties on all five free parameters can be found in Table. 2.

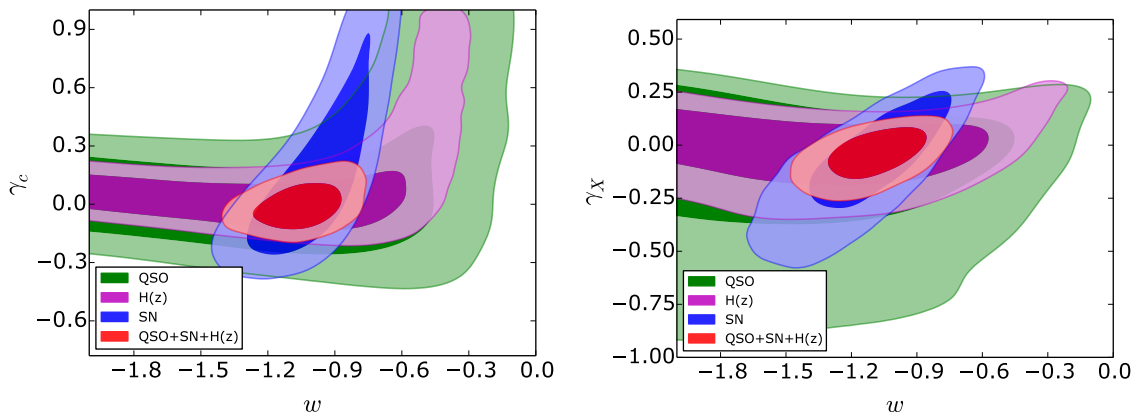


**Figure 1.**  $1\sigma$  and  $2\sigma$  confidence regions in the  $(w, \gamma_i)$  for the  $\gamma_c$ IwCDM model (left panel) and  $\gamma_X$ IwCDM model (right panel), which are derived from three different types of standard probes (QSO, SN and  $H(z)$ ).

In the first case of  $\gamma_c$ IwCDM model, in order to illustrate the performance of the quasar data compare with the statistical rulers, constraints from statistical standard rulers (CMB+BAO) and the joint constraint enriched with quasars (QSO+CMB+BAO) are

given in the left panel of Fig. 2. The right panel of Fig. 2 shows the confidence contours of model parameters constrained with the full combination of three types of standard probes (QSO+CMB+BAO+SN+ $H(z)$ ) and the combination excluding QSO data (CMB+BAO+SN+ $H(z)$ ). One can clearly see that the currently compiled quasar data improves the constraints on model parameters significantly. From the above results, the parameter  $\gamma_c$  capturing the interaction between DE and DM seems to be vanishing or slightly smaller than 0, which has been noticed by using the 182 Gold SNIa together with CMB and large-scale structure for the interacting holographic DE model [42] and by using the revised Hubble parameter data together with CMB and BAO [18]. The sample of 59 high redshift calibrated Gamma-Ray Burst (GRB) data, whose redshift region is more comparable to our quasar data, combined with BAO observation from SDSS and CMB from the 7-Year Wilkinson Microwave Anisotropy Probe (WMAP7) also support this result [21].

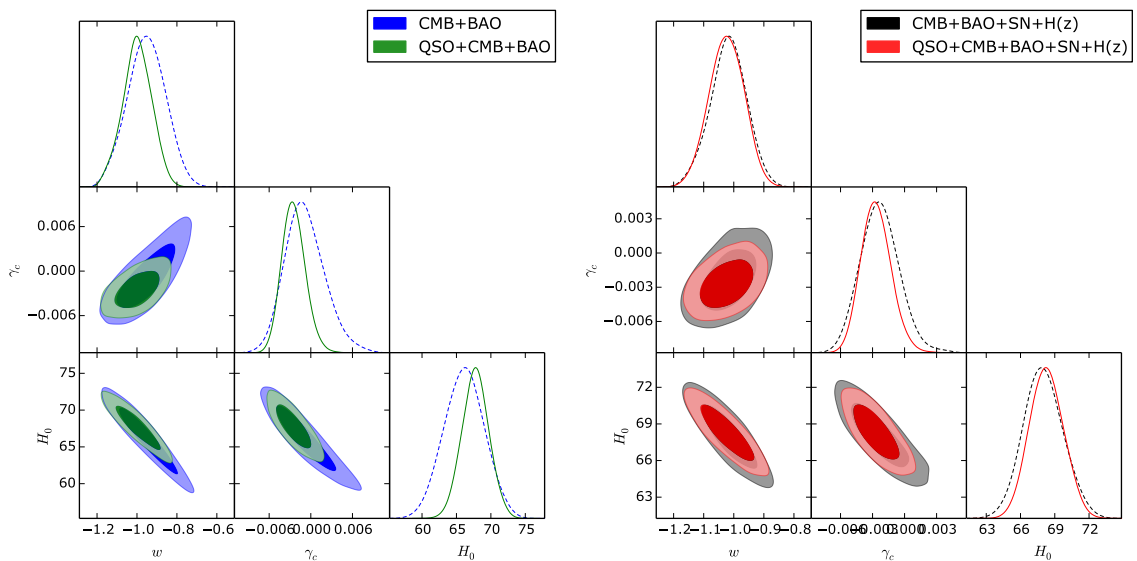


**Figure 2.** The 2-D plots and 1-D marginalized distributions with 1- $\sigma$  and 2- $\sigma$  contours of the  $\gamma_c$ IwCDM model parameters ( $w$ ,  $\gamma_c$ , and  $H_0$ ) obtained with the statistical standard rulers (CMB+BAO), combined standard rulers (QSO+CMB+BAO), combination of the standard probes (CMB+BAO+SN+ $H(z)$ ), and all probes including quasars (QSO+CMB+BAO+SN+ $H(z)$ ).

Concerning the  $\gamma_X$ IwCDM model when the interaction is proportional to the dark energy density  $\rho_X$ , comparison of the constraints obtained with statistical standard rulers and combined standard ruler including quasars indicate that quasar data can improve the final result noticeably. However, when SN Ia and  $H(z)$  data are included the influence of quasars is very small. This can change when bigger samples of quasar are available in the future. From the fitting results shown in Fig. 3 and Table. 2, the joint analysis provides a small negative coupling which agrees with the results by using the Gold SNIa together with CMB and large-scale structure for other interacting DE models describing the interaction in proportional to the DM energy density [14]. In addition, the constraining results in this work with the joint observational data including quasars are more stringent than previous results for constraining  $\gamma_X$ IDE model parameters with other combined observations arising from the

182 Gold SNe Ia samples, the shift parameter of CMB given by the WMAP3 observations, the BAO measurement from the Sloan Digital Sky Survey, the age estimates of 35 galaxies [19] and the 13  $H(z)$  measurements from the differential ages of red-envelope galaxies as well as the BAO peaks [18]. Similar conclusions could also be obtained from the  $\gamma_X$ I $\Lambda$ CDM model with  $w = -1$ , with the estimation of these cosmic parameters briefly summarized in Table. 2.

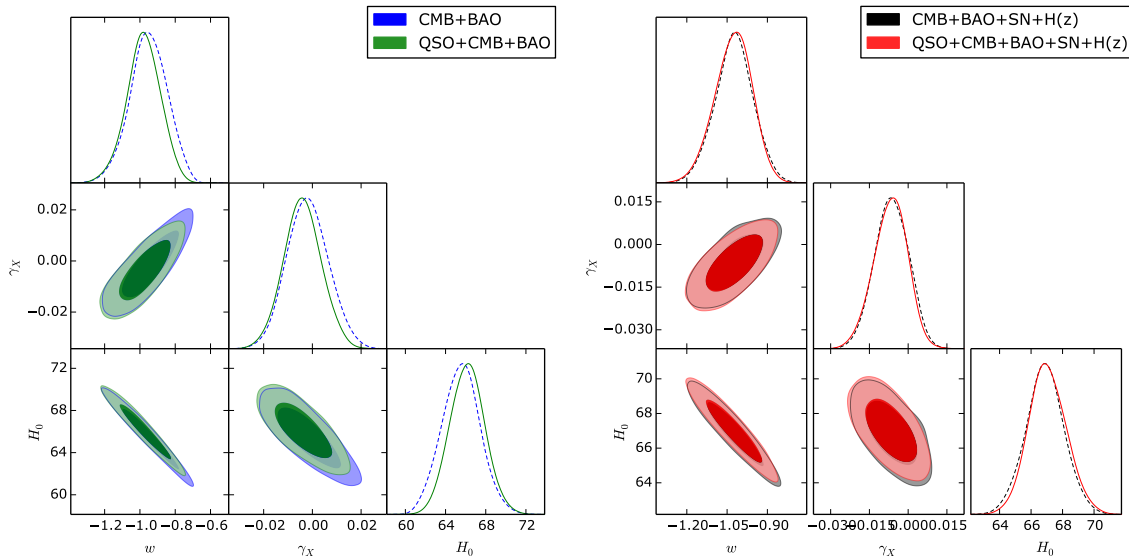


**Figure 3.** The same as Fig. 2, but for the  $\gamma_X$ IwCDM model.

Now it is worthwhile to make some comments on the results obtained above. Firstly, let us note that, following Cao et al. [25], we added extra 10% uncertainties to the observed angular sizes. This additional uncertainty is equivalent to adding an analogous 10% uncertainty in the linear size and affects the  $\chi^2$  minimization method making it increase after including QSO to joint analysis. It means that even though the linear sizes show negligible dependence on the luminosity and redshift, uncertainty of the  $l_m$  parameters can still be an important source of systematic errors. In particular, the calibration method for the linear size may also influence the goodness of the final result. Secondly, concerning the interaction term between dark energy and dark matter, the statistical analysis based on three types of standard probes demonstrates that the parameter describing the interaction between DE and DM seems to be vanishing or slightly smaller than zero. This conclusion is consistent with the previous results for constraining IDE model parameters with other combined observations. Thirdly, the estimated values of the Hubble constant are in agreement with the standard ones reported by *Planck* [9]. However, we still find strong degeneracies between  $\gamma_i$  and  $H_0$ , i.e., a negative value of interaction term will lead to a larger value of the Hubble constant, which may alleviate the tension of  $H_0$  between the recent *Planck* and *HST* measurements.

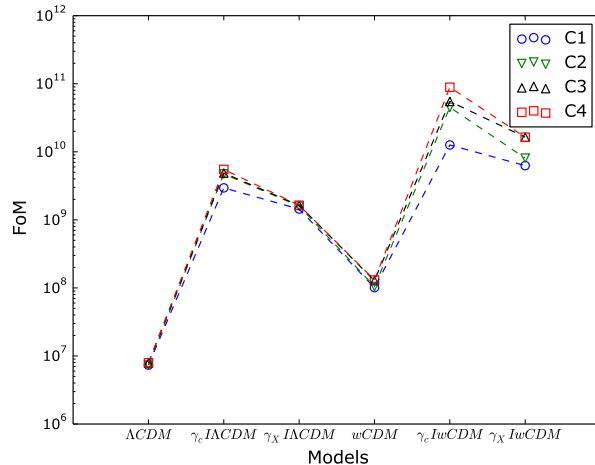


**Figure 4.** The FoM value for each cosmological model calculated from different data combinations: C1 (CMB+BAO), C2 (QSO+CMB+BAO), C3 (CMB+BAO+SN+ $H(z)$ ) and C4 (QSO+CMB+BAO+SN+ $H(z)$ ).

Finally, we would like to discuss statistically the performance of our data sets and perform model selection. On the one hand, in order to quantify the constraining power of the quasar data on cosmological model parameters, we calculate the Figure of Merit (FoM) for the IDE models with different data combinations. Based on the the previous definition proposed by the Dark Energy Task Force (DETF) for the CPL parametrization [43], a more general expression can be rewritten as [44]

$$FoM = (\det Cov(\mathbf{p}))^{-1/2} \quad (4.1)$$

where  $Cov(\mathbf{p})$  is the covariance matrix of relevant cosmological parameters  $\mathbf{p}$ . Higher value of the FoM is corresponds to tighter model constraint. From the results shown in Fig. 4 and Table 2, regarding the comparison between statistical standard rulers (CMB+BAO) and joint standard rulers (QSO+CMB+BAO), one can clearly see that the inclusion of the quasars sample will generate more stringent constraints on the  $\gamma_c IwCDM$  model. Comparison between the full combination (QSO+CMB+BAO+SN+ $H(z)$ ) and the combination excluding QSO data (CMB+BAO+SN+ $H(z)$ ) concerning FoM leads to similar conclusions. This can be understood in terms of a higher redshift range covered by QSOs in comparison to other astrophysical probes. However, for the rest of interacting dark energy models considered in this paper, the significance of this improvement is not evident and remains to be checked with a larger sample of quasars observed by VLBI at high angular resolutions [45].

On the other hand, in the face of so many competing interacting dark energy scenarios, it is important to find an effective way to decide which one is most favored by the data. Following the analysis of Biesiada [46] and Cao & Zhu [47], model comparison statistics including the Akaike Information Criterion (AIC) [48] and the Bayesian Information Criterion (BIC) [49] will be used for this purpose. The expression of the two main information criteria can be written as

$$AIC = -2\ln\mathcal{L}_{max} + 2k = \chi_{min}^2 + 2k \quad (4.2)$$

and

$$BIC = -2\ln\mathcal{L}_{max} + k\ln N = \chi_{min}^2 + k\ln N \quad (4.3)$$

where  $\mathcal{L}_{max} = \exp(-\chi_{min}^2/2)$  is the maximum likelihood value,  $k$  is the number of free parameters in the model and  $N$  is the total number of data points used in the statistical analysis.

Table 3 lists the AIC and BIC difference of each model. One can see that the two criteria lead to different conclusions, concerning the ranking of competing dark energy models. More specifically, according to the AIC, the  $\gamma_c\Lambda$ CDM performs the best, while the  $\gamma_X$ IwCDM model gets the smallest support from the current observations. On the contrary, the BIC criterion gives a different ranking: the cosmological constant model is still the best cosmological model. Then comes the sequence:  $\Lambda$ CDM,  $\gamma_c\Lambda$ CDM, and  $\gamma_X\Lambda$ CDM with one more free parameter, while  $\gamma_c$ IwCDM and  $\gamma_X$ IwCDM are clearly disfavored by the data. Therefore, our findings indicate that interacting dark energy models with more free parameters are substantially penalized by the BIC criterion, which agrees very well with the previous results derived from other cosmological probes including strong lensing systems [15, 47, 50].

**Table 3.** Summary of the information criteria for different interacting dark energy scenarios, obtained from the combinations of the data sets: C1 (CMB+BAO), C2 (QSO+CMB+BAO), C3 (CMB+BAO+SN+ $H(z)$ ) and C4 (QSO+CMB+BAO+SN+ $H(z)$ ). Corresponding results for the  $\Lambda$ CDM and wCDM models are also added for comparison.

Data	Model	$k$	AIC	$\Delta AIC$	BIC	$\Delta BIC$
C1 ( $N = 13$ )	$\Lambda$ CDM	3	16.35	0	18.04	0
	$\gamma_c\Lambda$ CDM	4	16.95	0.60	19.21	1.17
	$\gamma_X\Lambda$ CDM	4	17.16	0.81	19.42	1.38
	wCDM	4	16.86	0.51	19.12	1.08
	$\gamma_c$ IwCDM	5	18.76	2.41	21.58	3.54
	$\gamma_X$ IwCDM	5	18.85	2.50	21.67	3.63
C2 ( $N = 133$ )	$\Lambda$ CDM	3	370.55	1.36	379.22	0
	$\gamma_c\Lambda$ CDM	4	369.19	0	380.75	1.53
	$\gamma_X\Lambda$ CDM	4	371.24	2.05	382.80	3.58
	wCDM	4	371.29	2.10	382.85	3.63
	$\gamma_c$ IwCDM	5	371.19	2.00	385.64	6.42
	$\gamma_X$ IwCDM	5	373.13	3.94	387.58	8.36
C3 ( $N = 623$ )	$\Lambda$ CDM	3	577.26	0.14	590.56	0
	$\gamma_c\Lambda$ CDM	4	577.12	0	594.86	4.30
	$\gamma_X\Lambda$ CDM	4	578.04	0.92	595.78	5.22
	wCDM	4	578.96	1.84	596.70	6.14
	$\gamma_c$ IwCDM	5	579.07	1.95	601.24	10.68
	$\gamma_X$ IwCDM	5	579.97	2.85	602.14	11.58
C4 ( $N = 743$ )	$\Lambda$ CDM	3	931.36	1.98	945.19	0
	$\gamma_c\Lambda$ CDM	4	929.38	0	947.82	2.63
	$\gamma_X\Lambda$ CDM	4	932.07	2.15	950.51	5.32
	wCDM	4	933.13	3.75	951.57	6.38
	$\gamma_c$ IwCDM	5	931.16	1.78	954.21	9.02
	$\gamma_X$ IwCDM	5	933.94	4.56	956.99	11.80

## 5 Conclusions

In this paper, using the newly released data, derived from the very-long-baseline interferometry (VLBI) observations, comprising redshifts and angular sizes of compact structure in radio quasars, we have examined several popular phenomenological interaction models for dark energy and dark matter. Such models were proposed to alleviate the coincidence problem of the concordance  $\Lambda$ CDM model as well the tension between  $H_0$  derived from the recent *Planck* and *HST* measurements. The sub-sample of 120 intermediate-luminosity quasars in the redshift range of  $0.46 < z < 2.8$ , which was extracted from 613 milliarcsecond ultra-compact

radio sources observed by a 2.29 GHz VLBI all-sky survey, can be used as cosmological standard rulers with the linear sizes calibrated by a cosmological-model-independent method,  $l_m = 11.03 \pm 0.25$  pc. Compared with the SN Ia standard candles ( $z \sim 1.4$ ) extensively used in the cosmological study, the advantage of this data set is that quasars are observed at much higher redshifts ( $z \sim 3.0$ ), which motivate us to investigate the possible interaction between dark energy and dark matter at higher redshifts. To reduce the uncertainty and put tighter constraints on the coupling parameters, we added, in our discussion, the CMB results from the *Planck* as well as the BAO measurements both from the low- $z$  galaxy and higher- $z$  Lyman- $\alpha$  Forest (Ly $\alpha$ F) data. We expect that sensitivities of measurements of different observables can give complementary results on the coupling between dark sectors. Moreover, in order to quantify the constraining power of the current quasar data on the model parameters and the ranking of competing dark energy models, we assessed the FoM and performed model comparison using information-theoretical techniques (AIC and BIC criteria). Here we summarize our main conclusions in more detail:

- The quasar data could provide constraints competitive to the other two types of standard probes, i.e., the SNIa as standard candles with more precise data points and cosmic chronometers providing  $H(z)$  which are more directly related to the cosmological model parameters of interest. Moreover, our results strongly suggest that larger and more accurate sample of the quasar data can become an important complementary probe to test the properties of dark energy and break the degeneracy in the IDE model parameters. This conclusion is strengthened by the statistical results from the Figure of Merit, which supports the claim that the inclusion of the QSO sample covering higher redshift range leads to more stringent constraints on certain interacting dark energy models (especially the  $\gamma_c$ IwCDM model).
- The estimated values of the Hubble constant are in agreement with the standard ones reported by *Planck* [9]. However, strong degeneracies between  $\gamma_i$  and  $H_0$  implying that negative value of the interaction term will lead to a larger value of the Hubble constant, may alleviate the tension between the recent *Planck* and *HST* measurements of  $H_0$ .
- The AIC and BIC have provided quite different conclusions, concerning the ranking of competing dark energy models. More specifically, according to the AIC, the  $\gamma_c$ IACDM performs the best, while the  $\gamma_X$ IwCDM model gets the smallest support from the current observations. On the contrary, the BIC criterion gives a different ranking: the cosmological constant model is still the best cosmological model followed by the  $w$ CDM,  $\gamma_c$ IACDM, and  $\gamma_X$ IACDM, while  $\gamma_c$ IwCDM and  $\gamma_X$ IwCDM are clearly disfavored by the data. Therefore, our findings indicate that interacting dark energy models with more free parameters are substantially penalized by the BIC criterion, which agrees very well with the previous results derived from other cosmological probes.

## 6 Acknowledgments

This work was supported by the National Key Research and Development Program of China under Grants No. 2017YFA0402603; the Ministry of Science and Technology National Basic Science Program (Project 973) under Grants No. 2014CB845806; the National Natural Science Foundation of China under Grants Nos. 11503001, 11373014, and 11690023; the Fundamental Research Funds for the Central Universities and Scientific Research Foundation of Beijing Normal University; China Postdoctoral Science Foundation under grant No.



2015T80052; and the Opening Project of Key Laboratory of Computational Astrophysics, National Astronomical Observatories, Chinese Academy of Sciences. X.Z. is supported by the China Scholarship Council. M.B. gratefully acknowledges support and hospitality of the Beijing Normal University.

## References

- [1] Perlmutter, S., Aldering, G., Goldhaber, G., et al. 1999, ApJ, 517, 565
- [2] Riess, A. G., Filippenko, A. V., Challis, P., et al. 1998, AJ, 116, 1009
- [3] Eisenstein, D. J., Zehavi, I., Hogg, D. W., et al. 2005, ApJ, 633, 560
- [4] Komatsu, E., Smith, K. M., Dunkley, J., et al. 2011, ApJS, 192, 18
- [5] Sahni, V., Shafieloo, A., & Starobinsky, A. A. 2014, ApJ, 793, L40
- [6] Ding, X. H., Biesiada, M., Cao, S., Li, Z. X., & Zhu, Z. H., 2015, ApJ, 803, L22
- [7] Zheng, X. G., Ding, X. H., Biesiada, M., Cao, S., & Zhu, Z. H. 2016, ApJ, 825, 17
- [8] Riess, A. G., Macri, L. M., Hoffmann, S. L., et al. 2016, ApJ, 826, 56
- [9] Ade, P. A. R., et al. [Planck Collaboration] 2016, A&A, 594, A13
- [10] Amendola, L. 2000, PRD, 62, 043511
- [11] Olivares, G., Atrio-Barandela, F., & Pavon, D. 2006, PRD, 74
- [12] Wang, B., Abdalla, E., Atrio-Barandela, F., & Pavon, D. 2016, ROPP, 79, 096901 [arXiv:1603.08299]
- [13] Dalal, N., Abazajian, K., Jenkins, E., et al. 2001, PRL, 87, 141302
- [14] Guo, Z. K., Ohta, N., & Tsujikawa, S. 2007, PRD, 76, 023508
- [15] Li, X. L., Cao, S., Zheng, X. G., Li, S., & Biesiada, M. 2016, RAA, 16, 84
- [16] Will, C. M. 2001, Living Rev. Rel. 4, 4
- [17] Cao, S., Chen, Y., Zhang, J., & Ma, Y. B. 2015a, IJTP, 54, 1492
- [18] Cao, S., & Liang, N. 2013, IJMPD, 22, 1350082
- [19] Feng, C., Wang, B., Abdalla, E., & Su, R. 2008, PLB, 665, 118
- [20] Cao, S., Liang, N., & Zhu, Z.-H. 2011, MNRAS, 416, 1099
- [21] Pan, Y., Cao, S., Gong, Y.-G., Liao, K., & Zhu, Z.-H. 2013, PLB, 718, 699
- [22] Xia, D. M., & Wai, S. 2016, MNRAS, 463, 952
- [23] Costa, A. A., Xu, X. D., Wang, B., & Abdalla, E. 2017, JCAP, 01, 028
- [24] Cao, S., Biesiada, M., Jackson, J., Zheng, X. G., Zhao, Y. H., & Zhu, Z.-H. 2017a, JCAP, 02, 12
- [25] Cao, S., Zheng, X. G., Biesiada, M., et al. 2017b, A&A, 606, A15
- [26] Komatsu, E., et al. [WMAP Collaboration], 2009, AJS, 180, 330
- [27] Ade, P. A. R., et al. [Planck Collaboration] 2016, A&A, 594, A14
- [28] Gurvits, L. I. 1994, ApJ, 425, 442
- [29] Gurvits, L. I., Kellerman, K. I. & Frey, S. 1999, A&A, 342, 378
- [30] Vishwakarma, R. G. 2001, Classical Quantum Gravity, 18, 1159
- [31] Cao, S., Biesiada, M., Zheng, X. & Zhu, Z.-H. 2015b, ApJ, 806, 66
- [32] Preston, R. A., Morabito, D. D., Williams, J. G., et al. 1985, AJ, 90, 1599

- [33] Hu, W., & Sugiyama, N. 1996, ApJ, 471, 542
- [34] Bond, J. R., Efstathiou, G., & Tegmark, M., 1997, MNRAS, 291, L33
- [35] Beutler, F., Blake, C., Colless, M., et al., 2011, MNRAS, 416, 3017 [arXiv:1106.3366]
- [36] Ross, A. J., Samushia, L., Howlett, C., et al. 2015, MNRAS, 449, 835
- [37] Anderson, L., Aubourg, E., Bailey, S., et al. 2014, MNRAS, 441, 24
- [38] Bautista, J. E., Busca, N. G., Guy, J., et al. 2017, A&A, in press [arXiv:1702.00176]
- [39] Eisenstein, D. J., & Hu, W. 1998, ApJ, 496, 605
- [40] Suzuki, N., Rubin, D., Lidman, C., et al. 2012, ApJ, 746, 85
- [41] Lewis, A., & Bridle, S. 2002, PRD, 66, 103
- [42] Feng, C., Wang, B., Gong, Y. G., & Su, R. K. 2007, JCAP, 09, 005
- [43] Albrecht, A., et al. 2006, Report of the Dark Energy Task Force [arXiv:0609591]
- [44] Wang Y. 2008, PRD, 77, 123525 [arXiv:0803.4295]
- [45] Pushkarev, A. B., & Kovalev, Y. Y. 2015, MNRAS, 452, 4274
- [46] Biesiada, M. 2007, JCAP, 02, 003
- [47] Cao, S., & Zhu, Z.-H. 2011, PRD, 84, 023005
- [48] Akaike, H. 1974, IEEE Transactions on Automatic Control, 716, 72, 3
- [49] Schwarz, G. 1978, Annals of Statistics, 15, 18
- [50] Biesiada, M., Piórkowska, A., & Malec, B. 2010, MNRAS, 406, 1055